Control of J_C anisotropy in REBCO thin films with nanoscale Y211 inclusions

Alok K. Jha, Kaname Matsumoto, Tomoya Horide
(Kyushu Institute of Technology)

Shrikant Saini, Paolo Mele
(Muroran Institute of Technology)

Ataru Ichinose
(CRIEPI)

Yutaka Yoshida
(Nagoya University)

Satoshi Awaji
(Tohoku University)

Sept. 20, 2017: Geneva

Outline:

- **Objective**

  Use of surface modified target approach to enhance the critical current density and also to control the anisotropic behavior of the J_C

- **The details of surface modified approach**

  The methodology employed and the expected microstructure and other transport properties

- **Results and discussion**

  Understanding the mechanism for control of J_C anisotropy in YBCO films using existing theoretical model/s.

- **Conclusion and future plan**

PLD Schematics

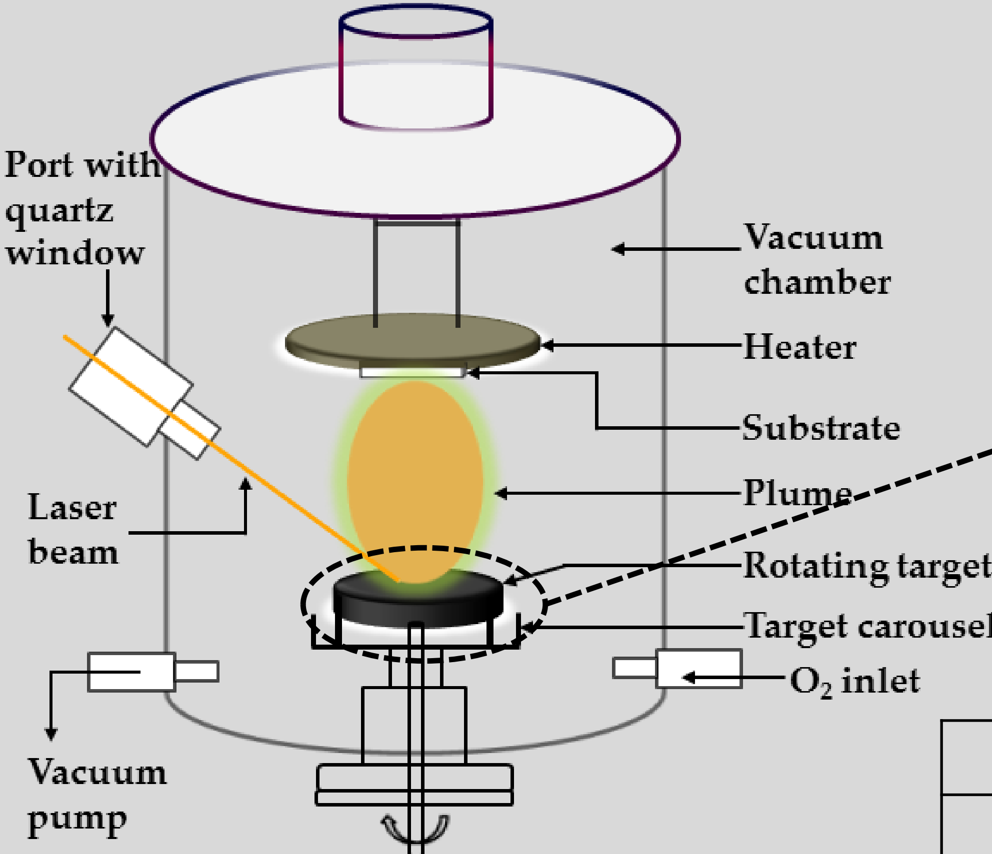

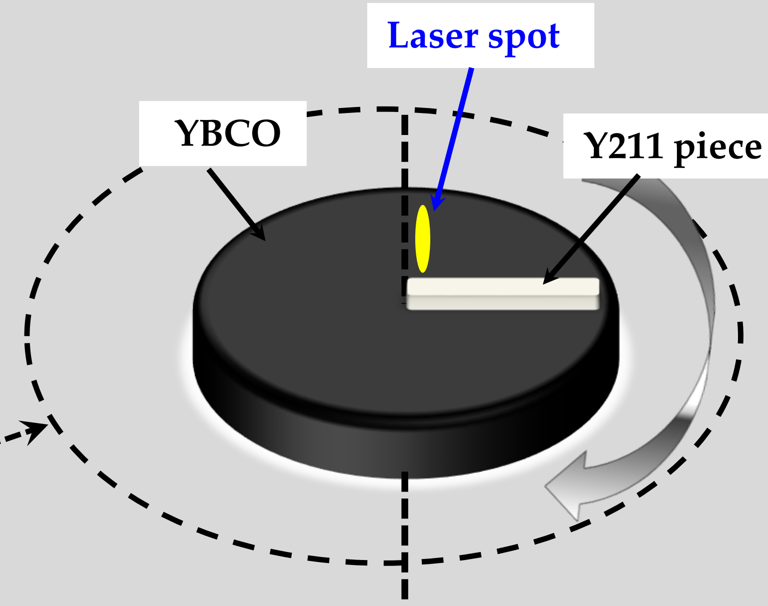

	Y211A	Y211B	Y211C
YBCO	1.8 area%	3.6 area%	5.4 area%

The area percentage was calculated by the relative ablation area from YBCO and Y211 portions

Microstructure

YBCO+Y211A

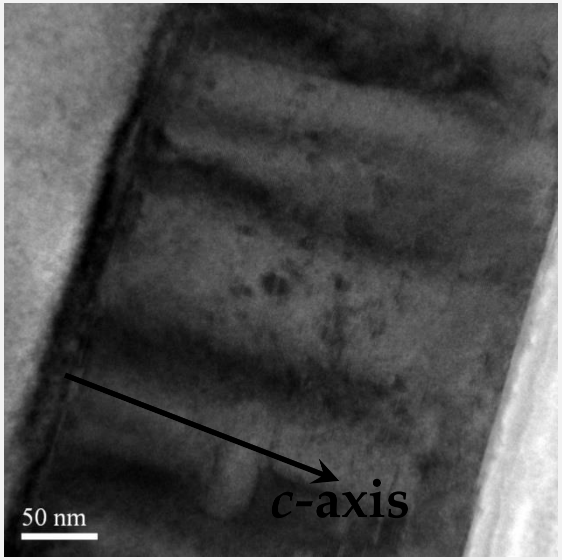

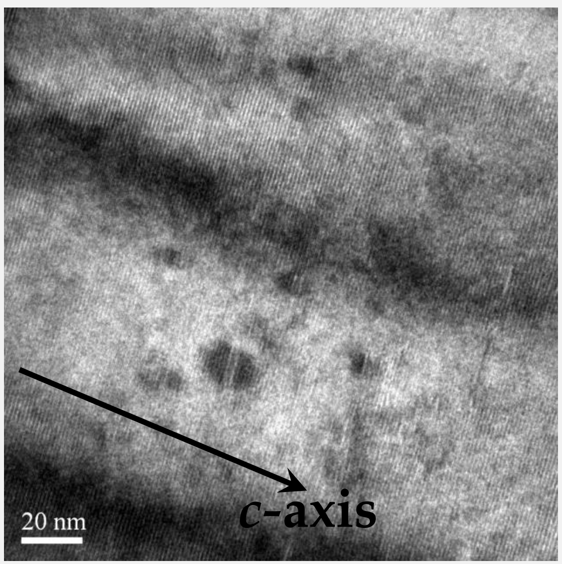

YBCO+Y211B

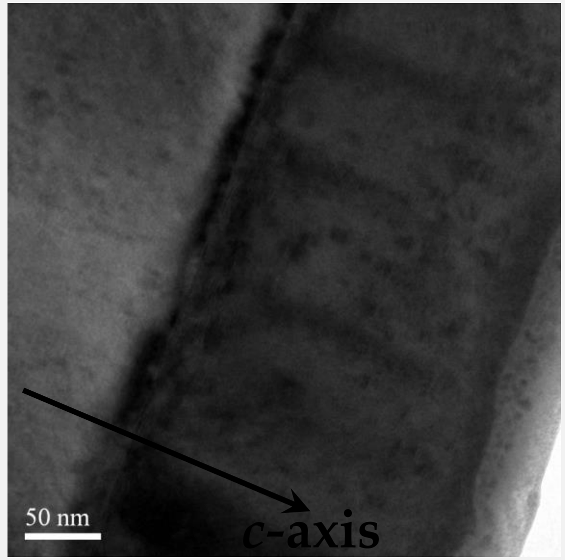

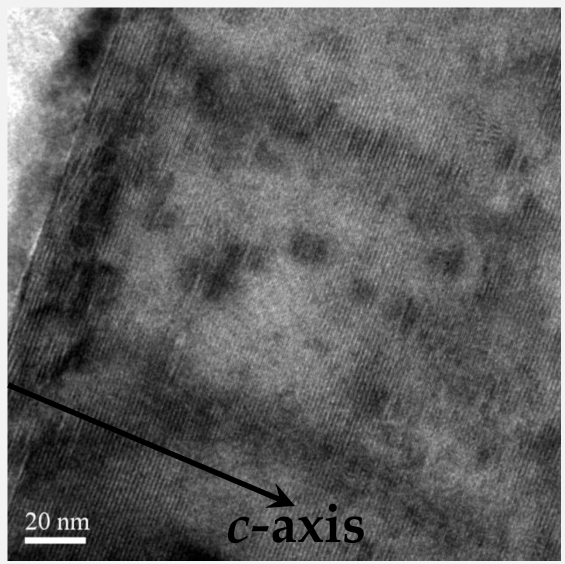

YBCO+Y211C

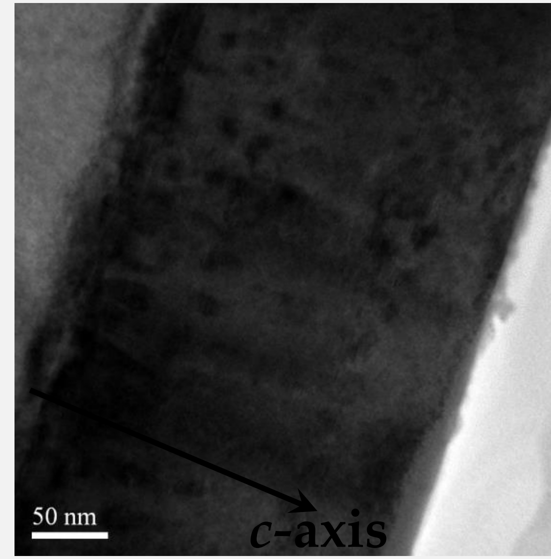

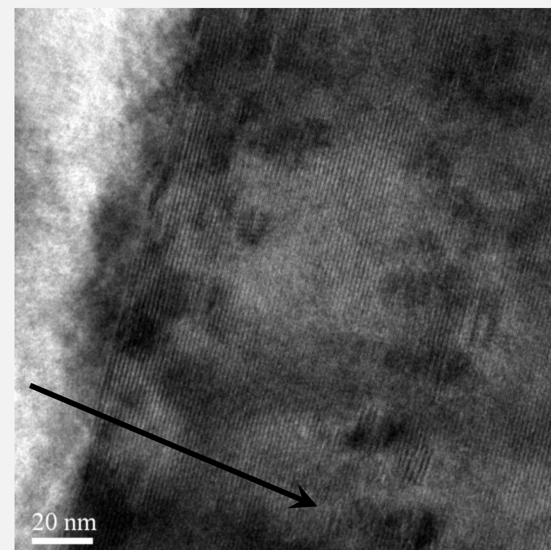

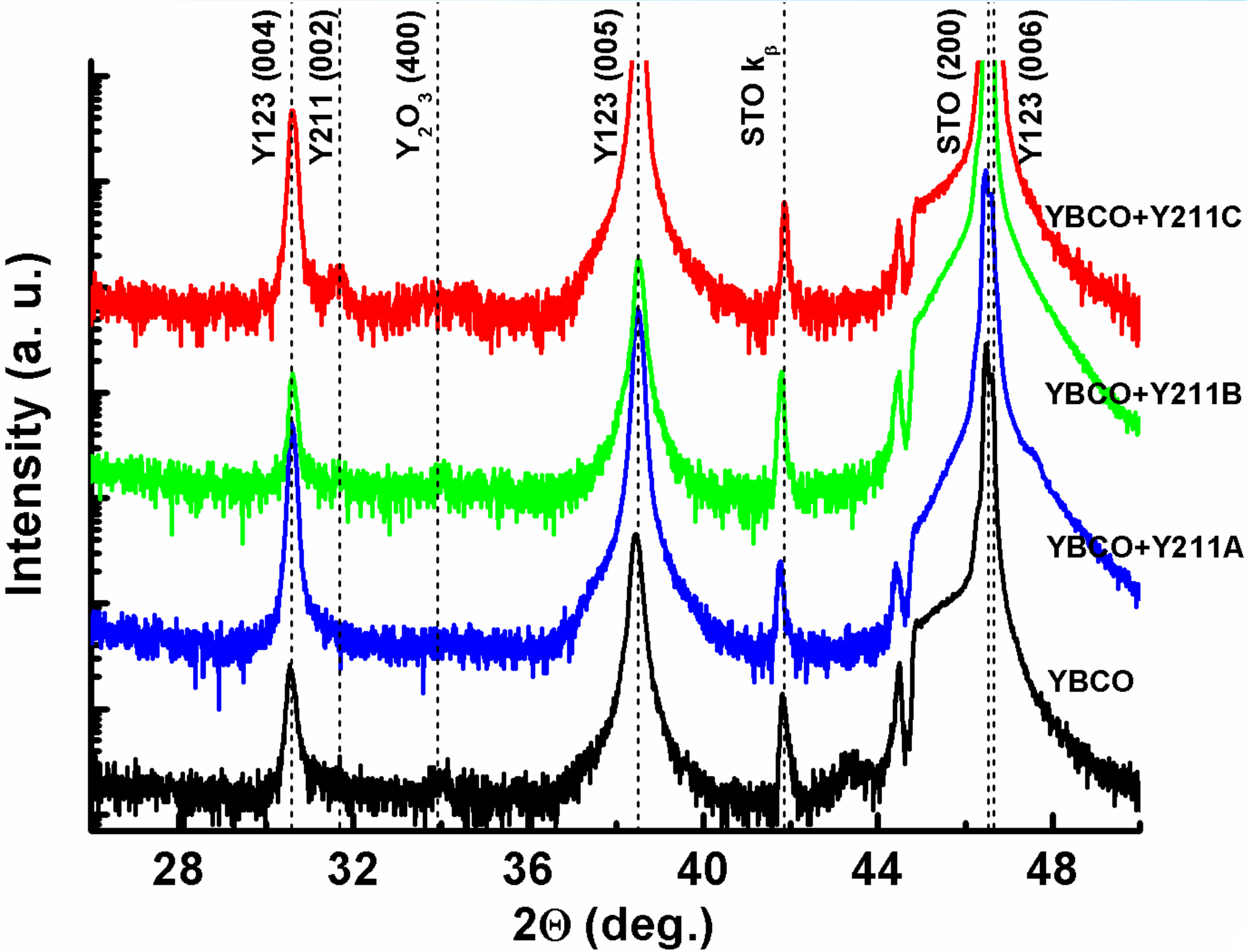

Y123 (004)
Y211 (002)
Y2O3 (400)
Y123 (005)
STO kβ
STO (200)
Y123 (006)
YBCO+Y211C
YBCO+Y211B
YBCO+Y211A
YBCO
Intensity (a. u.)
28
32
36
40
44
48
2Θ (deg.)

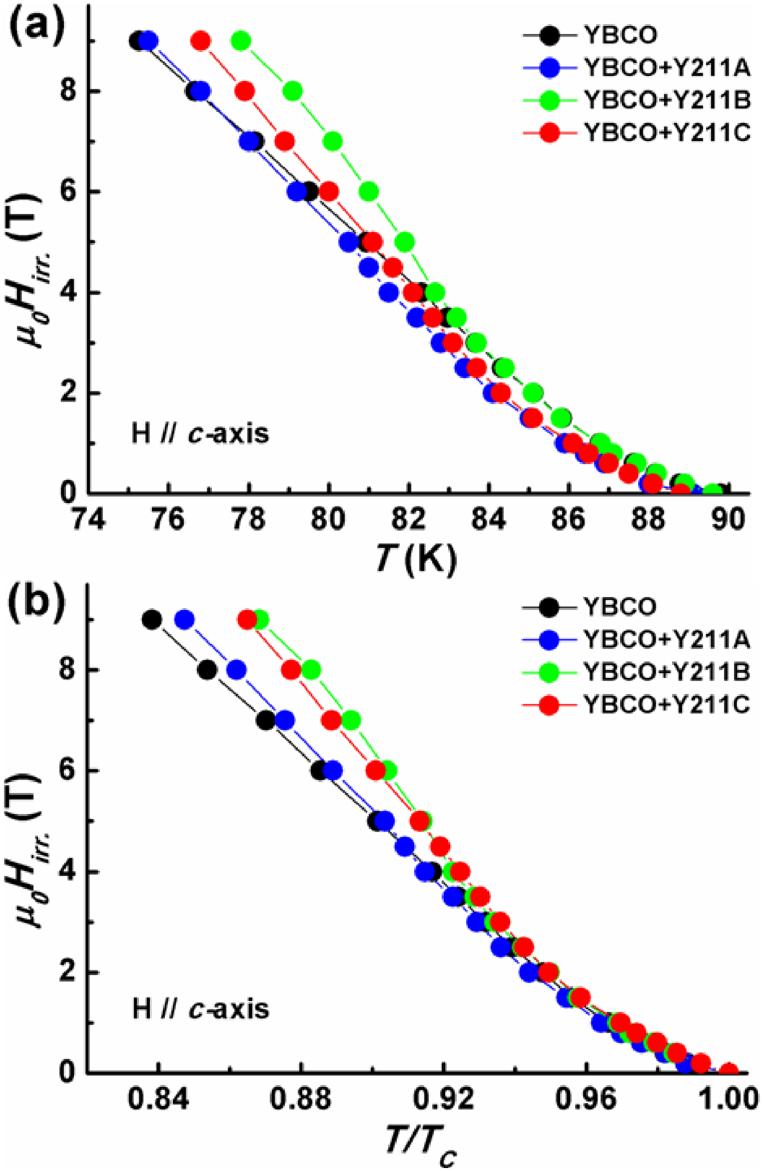

YBCO+Y211 A

YBCO+Y211 C

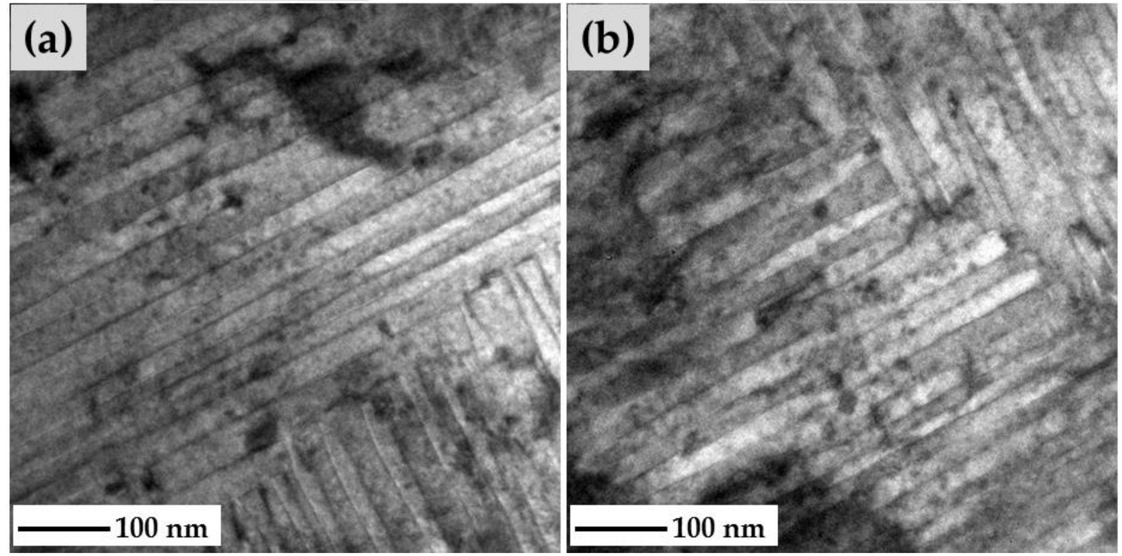

Low resolution planar view of the TEM image for the nanocomposite films

- There is pronounced up-shift in the irreversibility lines of YBCO+Y211 nanocomposite films.

- The shifting of the irreversibility lines towards higher H-T regime may be attributed to the cooperative contribution from twin-boundaries and the Y211.

J_C-B, F_p-B characteristics:

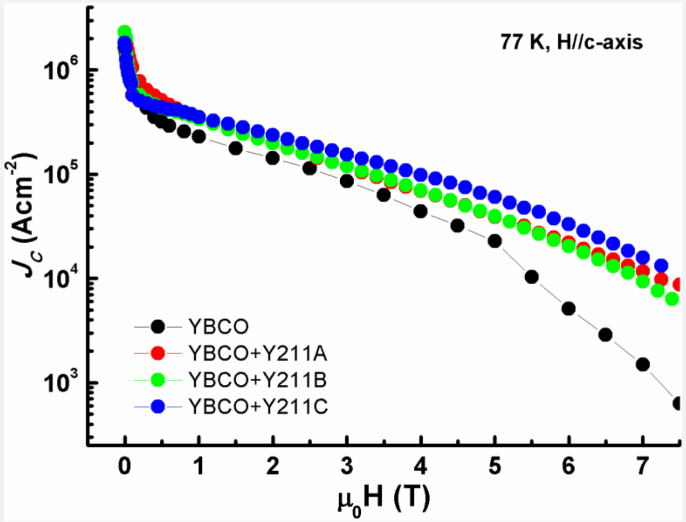

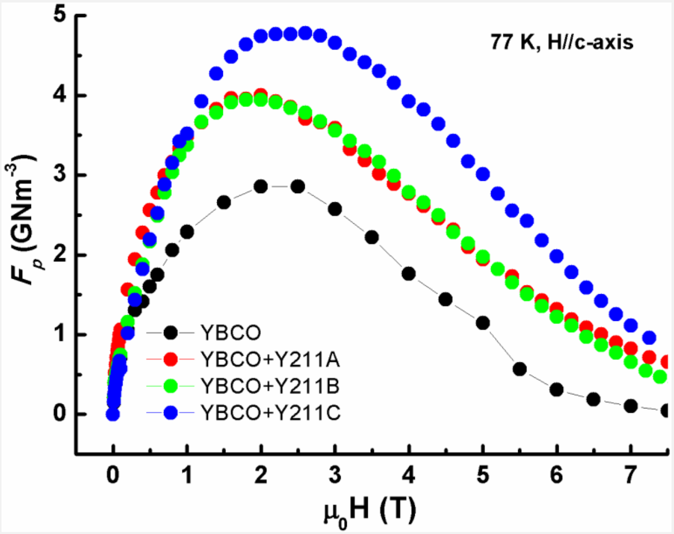

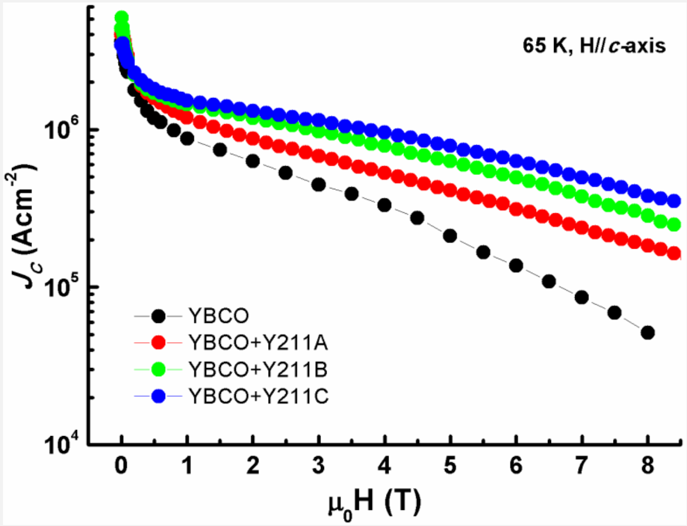

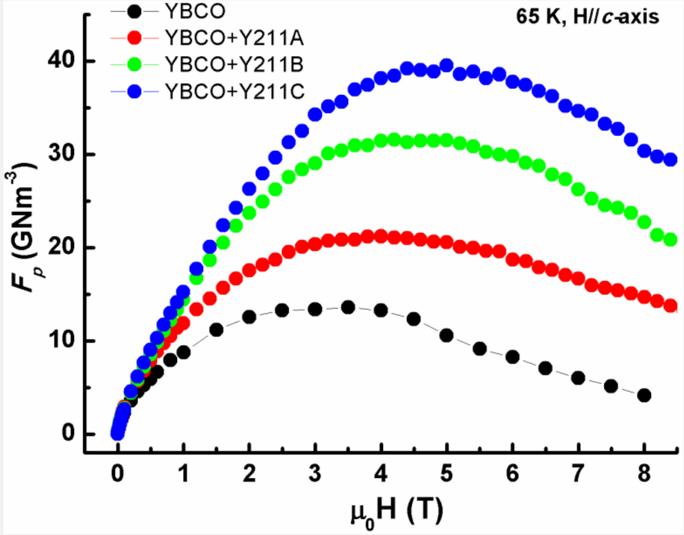

	77 K $F_{pmax.}$	65 K $F_{pmax.}$
YBCO	2.86	13.6
YBCO+Y211A	4.0	21.2
YBCO+Y211B	3.95	30.95
YBCO+Y211C	4.78	39.53

The $F_{pmax.}$ and $B_{max.}$ increases systematically as function of APC density in the thin films

Angular dependence of J_C @ 77 K: 1 T and 3 T

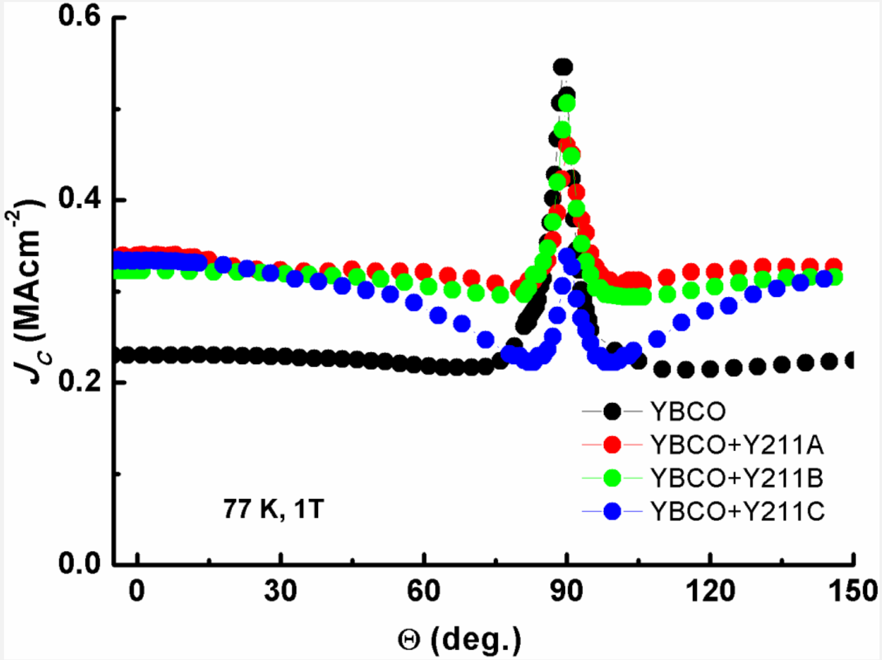

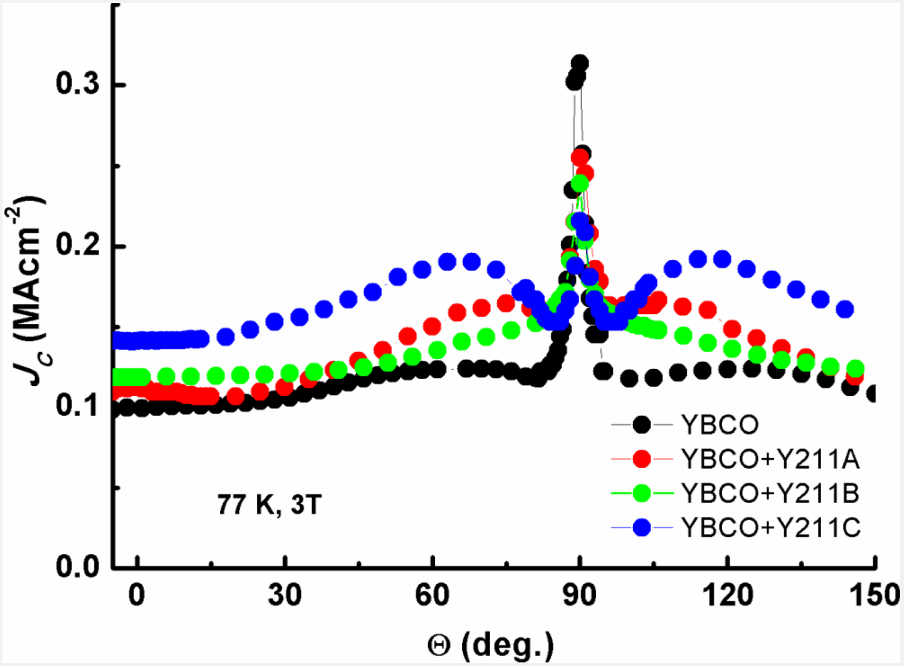

- **The enhancement of J_C in all the YBCO+Y211 composite samples is uniform over a broad angular range. However, at 77 K, 1 T; in YBCO+Y211C samples, there is a dip near the *ab*-plane and the *ab*-peak is also shortened.**

- **At 77 K, 3 T YBCO+Y211 samples exhibits systematic enhancement with respect to the Y211 nanoparticles density in the samples.**

Angular dependence of J_C @ 65 K: 1 T, 3 T and 5 T

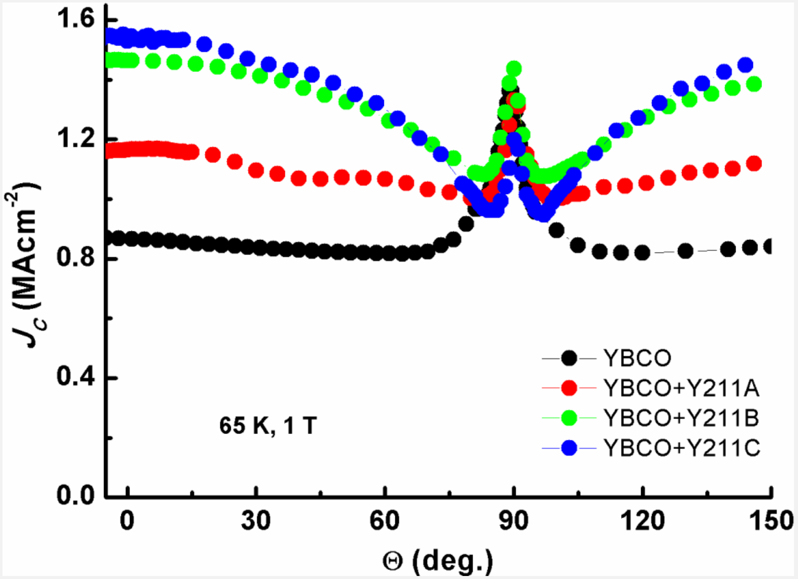

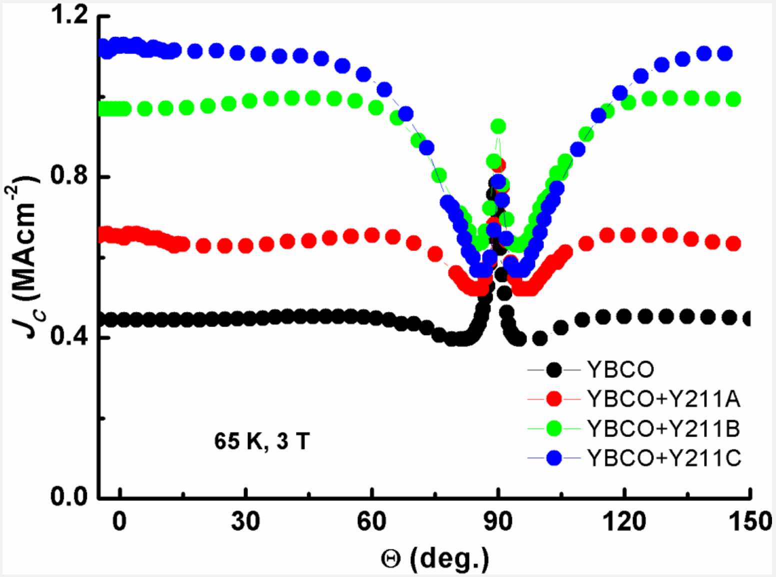

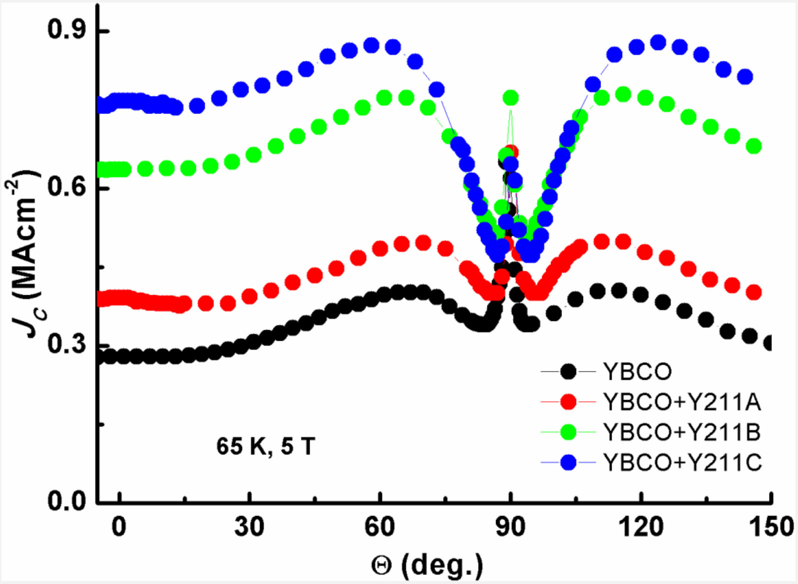

- The angular variation of J_C for YBCO+Y211 is unusually uniform over a broad angular range. However, there is sharp dip in J_C near *ab*-plane is also observed.

- YBCO+Y211 sample exhibits almost isotropic J_C behavior over a broad angular range which could have resulted from uniform distribution of Y211 nanoparticles across the sample.

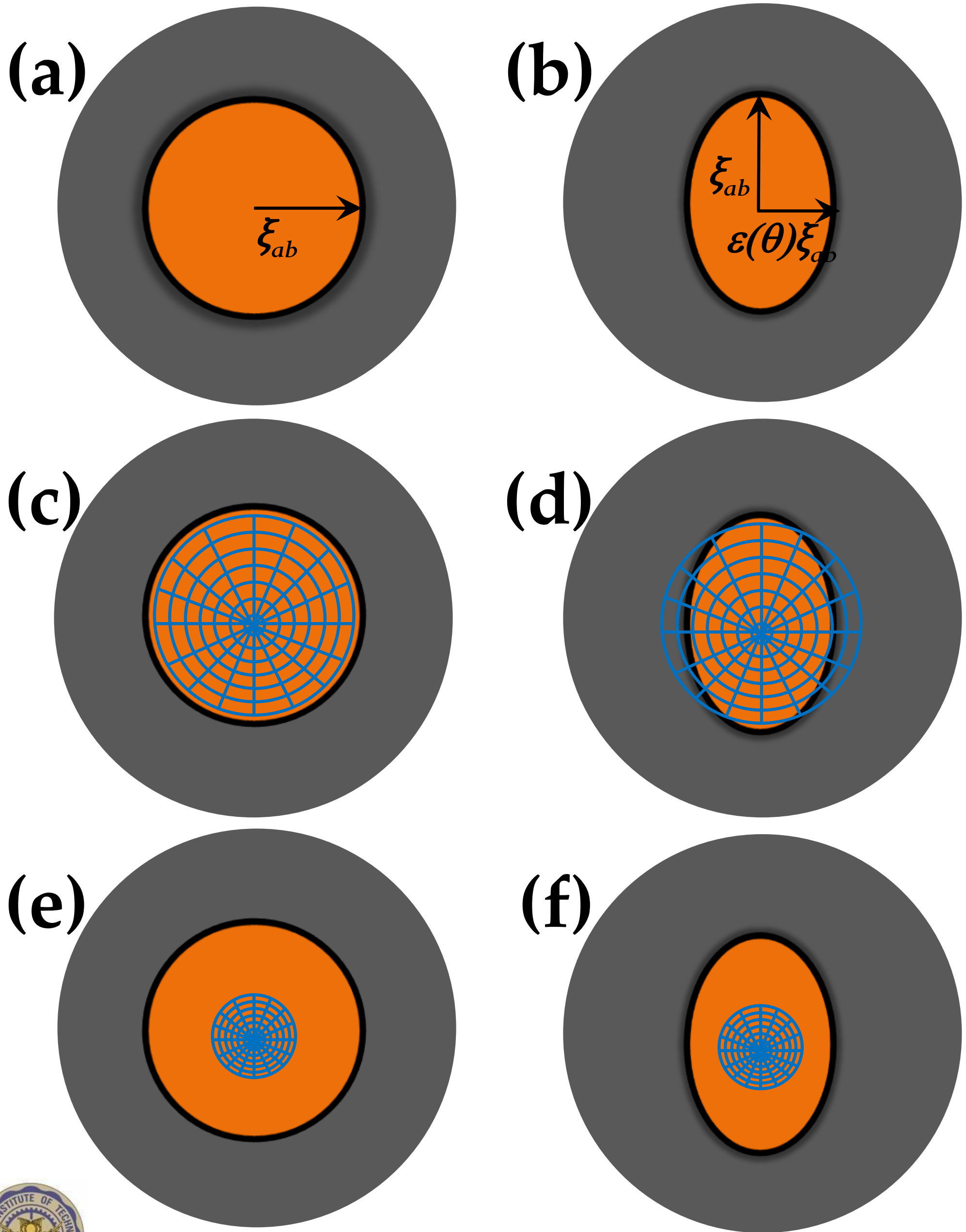

Significance of the size of a defect which pins a vortex core:

(a)shows an unpinned vortex core for $H_a \parallel c\text{-}axis$, while (b) illustrates the shrinkage of a vortex core with θ.

$$\varepsilon(\theta) = \sqrt{(cos^2\theta + \gamma^{-2} sin^2\theta)}$$

(c) and (d) show the change in the pinning energy From $E_p \propto \xi_{ab}^2 r_d$ to $\xi_{ab}^2 \varepsilon(\theta) r_d$ due to the interaction of a large defect (radius $\geq \xi_{ab}$) with the vortex core in each case.

(e) and (f) illustrate the constant pinning energy ($E_p \propto r_d^3$) when a small defect pins the vortex core.

V. Mishev *et al* SuST 28 (2015) 102001

Variation of pinning potential due to 3-D and 2-D defects

(a)

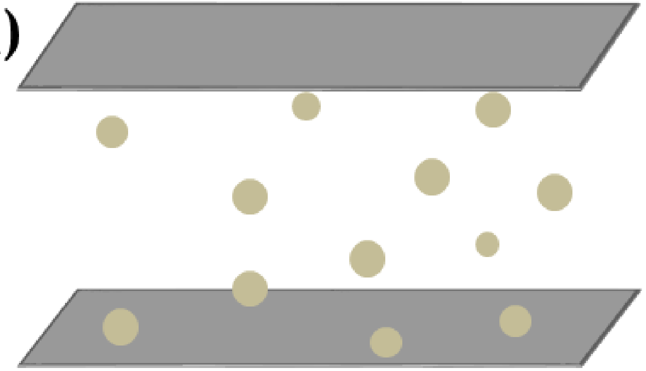

$$U_p = \left(\frac{B_c^2(T)}{2\mu_0}\right)\xi_{ab}\xi_{ab}(\theta)d$$

$$\xi_{ab}(\theta) = \xi_{ab}\varepsilon(\theta);$$

$$\varepsilon(\theta) = (cos^2\theta + \gamma^{-2}sin^2\theta)^{\frac{1}{2}}$$

$$B_c(T) = \frac{\phi_0}{2\sqrt{2\pi\xi_{ab}(T)\lambda_{ab}(T)}}$$

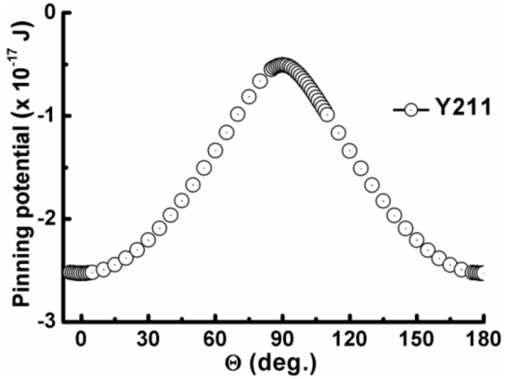

(b)

$$tan\theta_{acc.} = \sqrt{\frac{2u_p}{\varepsilon_l}}$$

$$\varepsilon_l = \frac{\phi_0^2}{4\pi\mu_0\lambda_{ab}^2}\ln\left(\frac{a_0}{\xi_{ab}}\right)$$

$$a_0 = \sqrt{\frac{\phi_0}{B}}$$

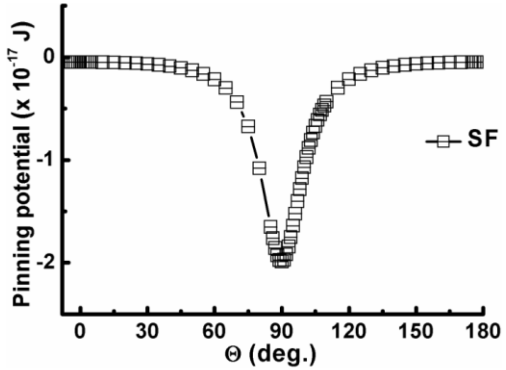

(c)

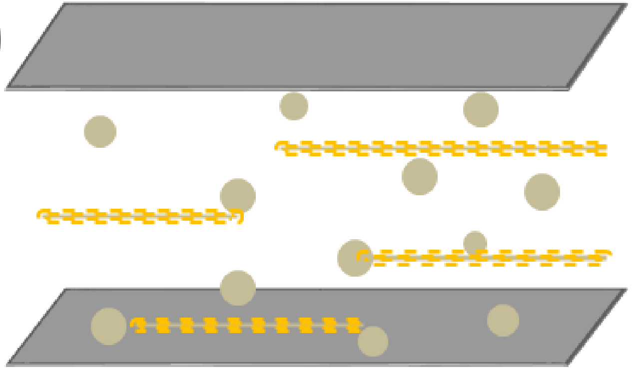

Combination of the two kinds of defects leads to the formation of crossover angle which reflects the region of dominance of different pinning landscapes

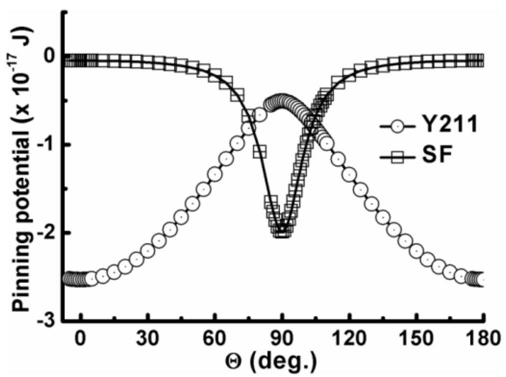

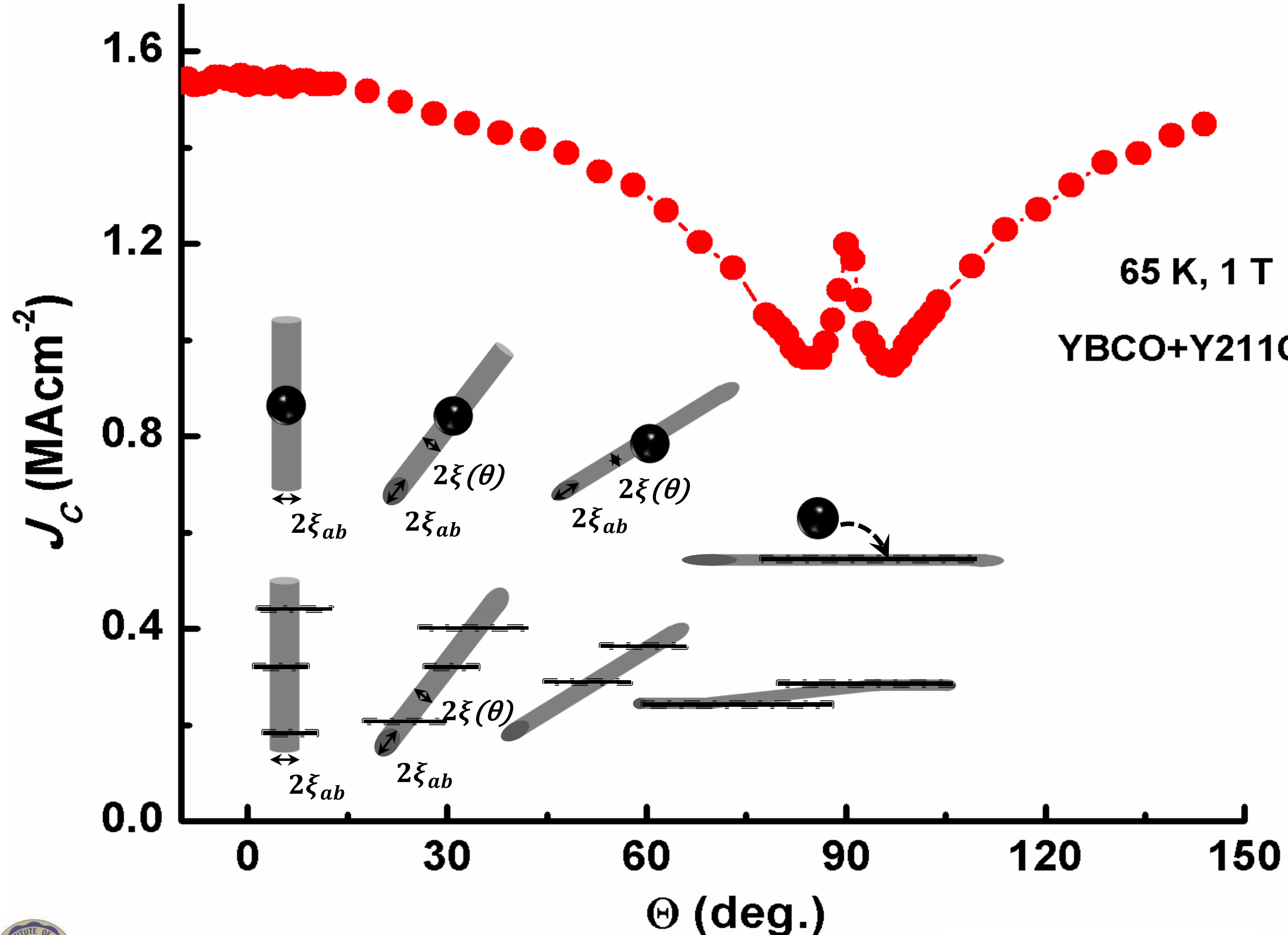

Jha *et al.* JAP (2017)

Conclusions:

- YBCO films incorporating 3-D APCs are prepared by surface modified target approach.

- $F_{pmax.}$ and $B_{max.}$ values are found to depend systematically on the concentration of hybrid APCs in the YBCO thin films

- Angular dependence of J_C shows systematic variation with respect to the APC concentration in the YBCO+Y211 films.

- Angular variation of J_C in YBCO+Y211 films were analyzed qualitatively in terms of pinning energy using standard theoretical models and the role of spherical and planar defect were explained.

Future plan:

- Different *RE*211 nanoinclusions will be attempted to see its effect on the angular dependent J_C behaviour.

- Further low temperature studies will be carried out in detail to understand the angular dependent J_C behavior at lower temperatures.

Thank you for your kind attention!